Supplementary Information

Liposome-based combination strategy of doxorubicin and PI3K inhibitor efficiently inhibits pre-metastatic initiation by acting on both tumor cells and tumor associated macrophages

Chaohui Luo, Minglu Zhou, Cheng Chen, Shujie Li, Qiuyi Li, Yuan Huang and Zhou Zhou*

Key Laboratory of Drug-Targeting and Drug Delivery System of the Education Ministry and Sichuan Province, Sichuan Engineering Laboratory for Plant -Sourced Drug and Sichuan Research Center for Drug Precision Industrial Technology, West China School of Pharmacy, Sichuan University, Chengdu 610041, China.

**Corresponding authorE-mail: zhou_zhou610@163.com*

Table S1. Characterization of liposomes

	Size (nm)	Zeta potential (mV)	PDI	EE (%)	DL (%)
PEG-Lip-Dox	118.97 ± 4.80	-21.20 ± 0.30	0.25 ± 0.01	97.06 ± 0.52	4.48 ± 0.01
PEG-Lip-C6	106.27± 0.81	-28.53 ± 0.25	0.27 ± 0.02	85.30 ± 3.21	0.12 ± 0.002
Lip-C6	123.27 ± 2.42	-21.20 ± 0.30	0.27 ± 0.01	88.83 ± 2.64	0.14 ± 0.002
PEG-Lip-DiR	109.00 ± 10.13	-17.83 ± 0.15	0.27 ± 0.03	89.90 ± 2.19	0.27 ± 0.004
Lip-DiR	111.70 ± 0.71	-13.27± 0.31	0.26 ± 0.03	90.18 ± 2.00	0.28 ± 0.01

Table S2. IC_{50} value of free drugs and liposomes (n=3).

	IC_{50} (μg/ml, Dox equiv)
Dox	0.618±0.05
Dox+LY	0.180±0.02
Lip-Dox	2.007±0.13
Combination	0.650±0.10

Table S3. Pharmacokinetic parameters of liposomes (n=3).

	$T_{1/2}$(h)	$AUC_{(0-\infty)}$ (mg/L*h)
Free C6	1.76 ± 0.57	7.33 ± 2.23
PEG-Lip-C6	6.39 ± 1.38	65.80 ± 8.16
Lip-C6	5.12 ± 0.31	62.67 ± 13.72

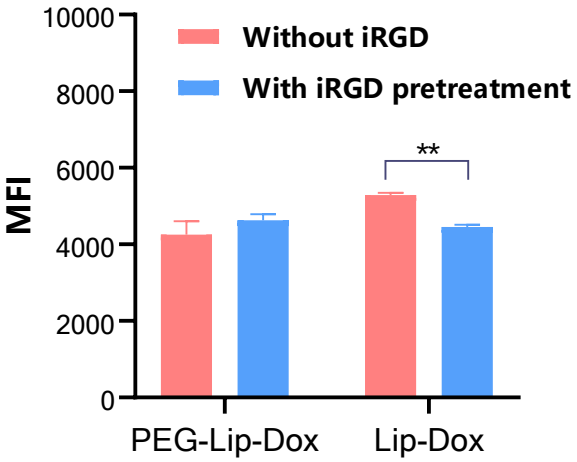

Fig.S1 Cellular uptake of PEG-Lip-Dox and Lip-Dox in 4T1 cells with iRGD peptide pretreatment (n = 3, $^{**}p < 0.01$).

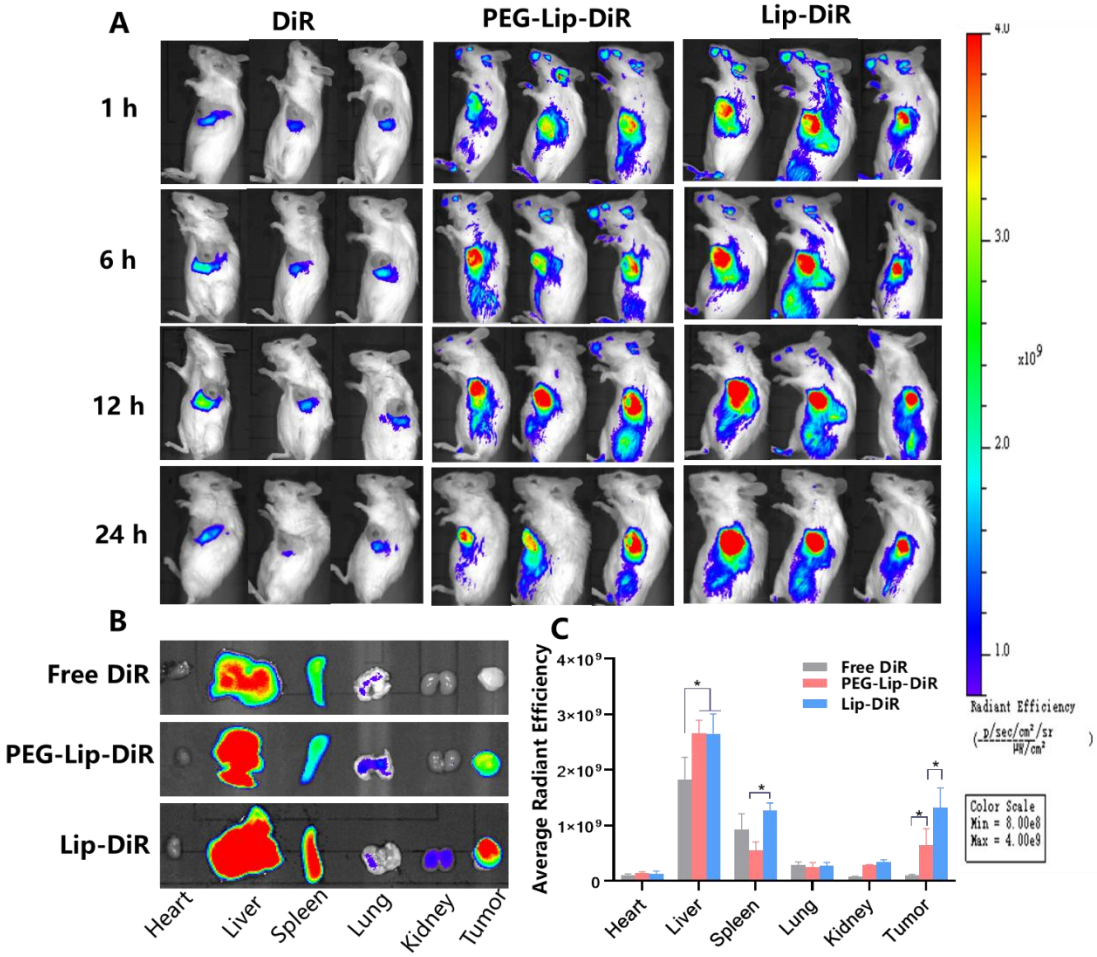

Fig.S2 *In vivo* biodistribution of liposomes. (A) fluorescence images showing the biodistribution of liposomes at different time points after injection of free DiR or DiR-loaded liposomes. (B) *Ex vivo* fluorescence images and (C) semiquantitative biodistribution analysis in major organs and tumors (n=3, *$p < 0.05$).

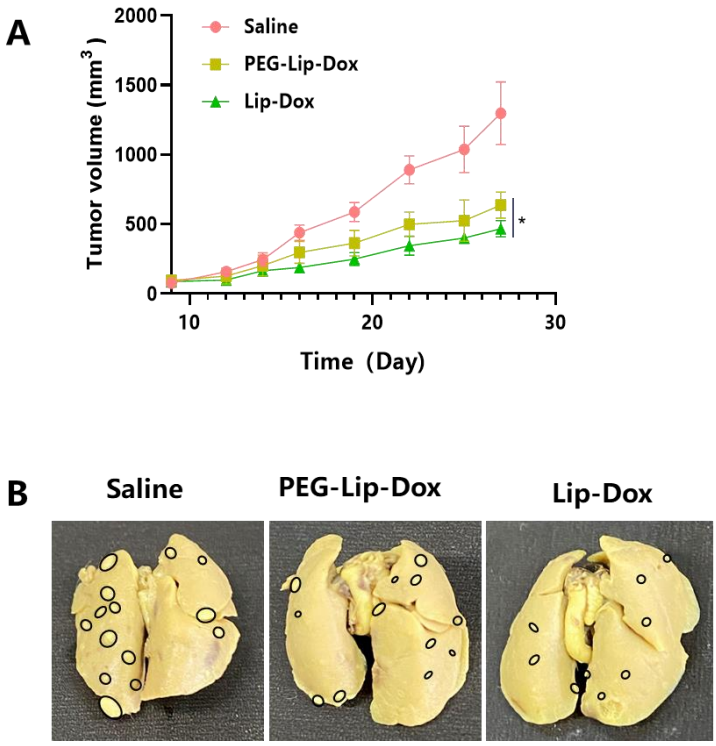

Fig. S3 Antitumor and anti-metastasis activity of Dox-loaded liposomes *in vivo*. (A) tumor growth curve of 4T1 tumor-bearing BALB/c mice after different Dox-loaded liposomes treatment (n=5, *$p < 0.05$). (B) Representative lung images of mice.

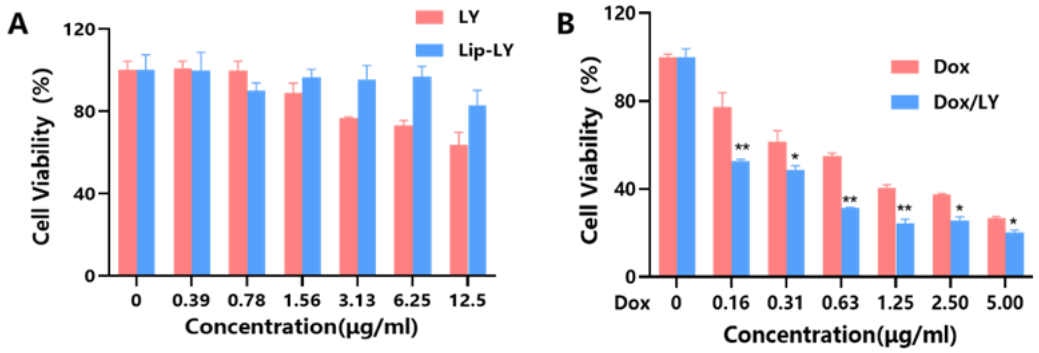

Fig. S4 Cell viability of 4T1 cells after indicated treatments. (A) Cell viability of LY and Lip-LY. (B) Cell viability of Dox and free combination. (n=3, *$p < 0.05$, **$p < 0.01$)

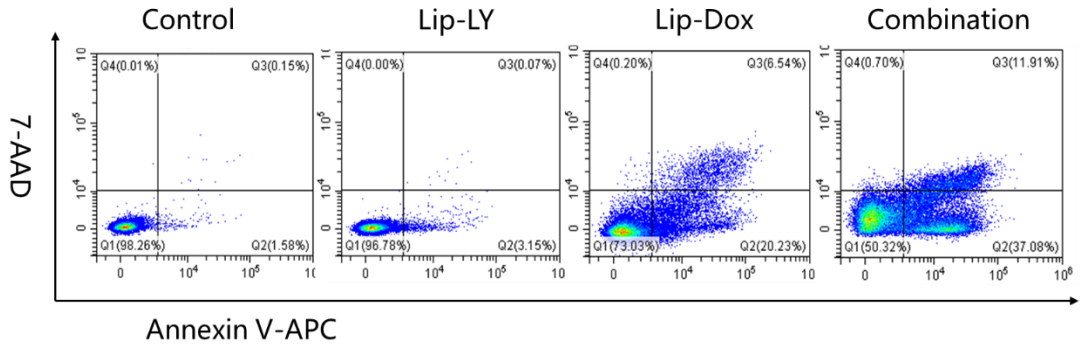

Fig. S5 Representative flow cytometry profiles of cell apoptosis in 4T1 cells after indicated treatments.

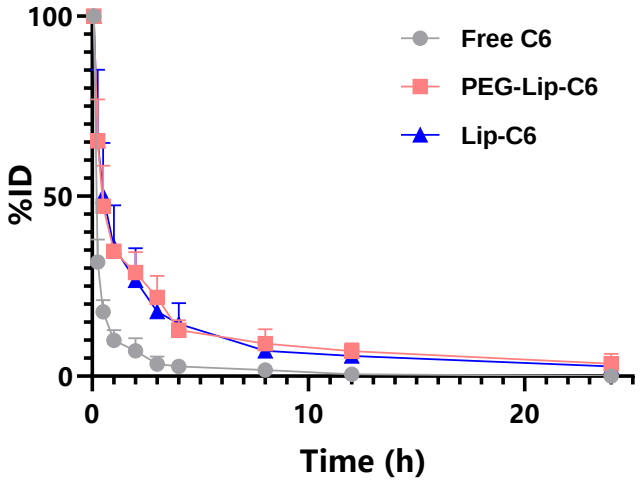

Fig. S6 Pharmacokinetics behaviors of liposomes (n=3).

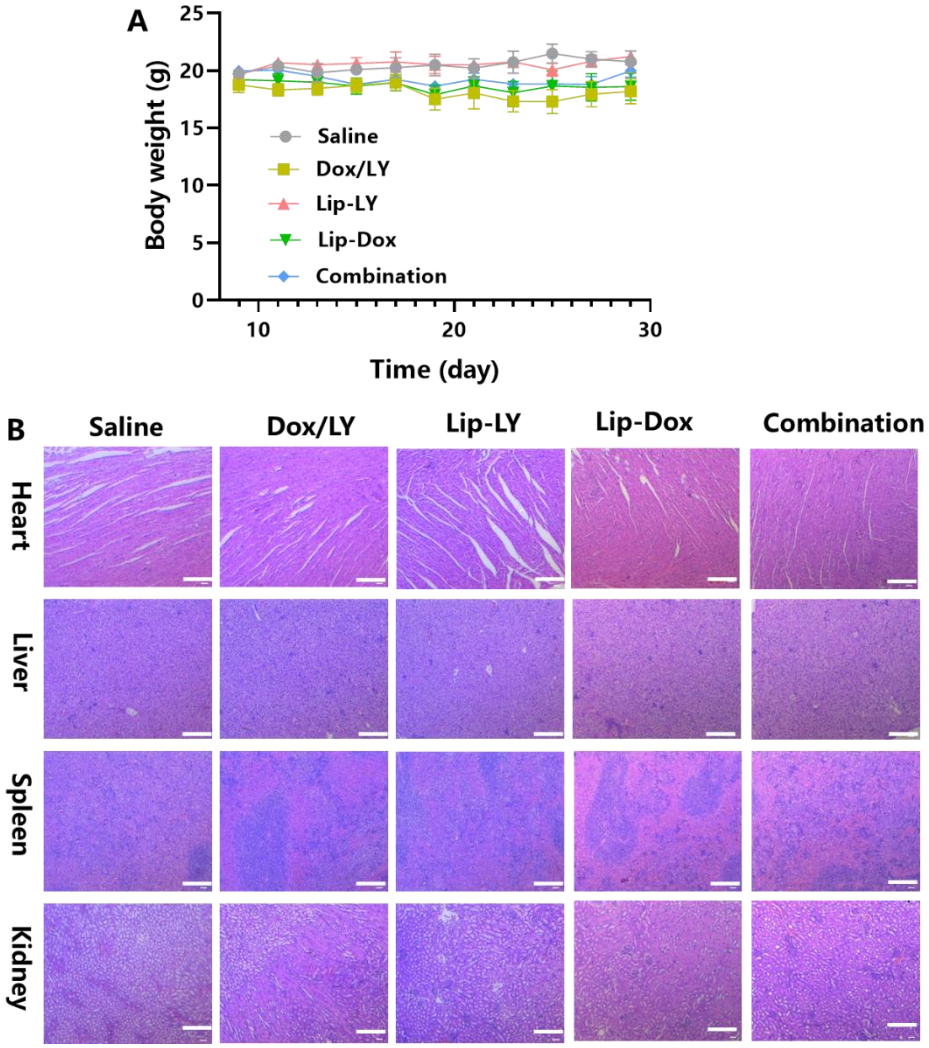

Fig.S7 Safety evaluation *in vivo*. (A) body weight of 4T1 tumor-bearing BALB/c mice (n=5). (B) H&E staining of major organs (scale bar: 100 μm).

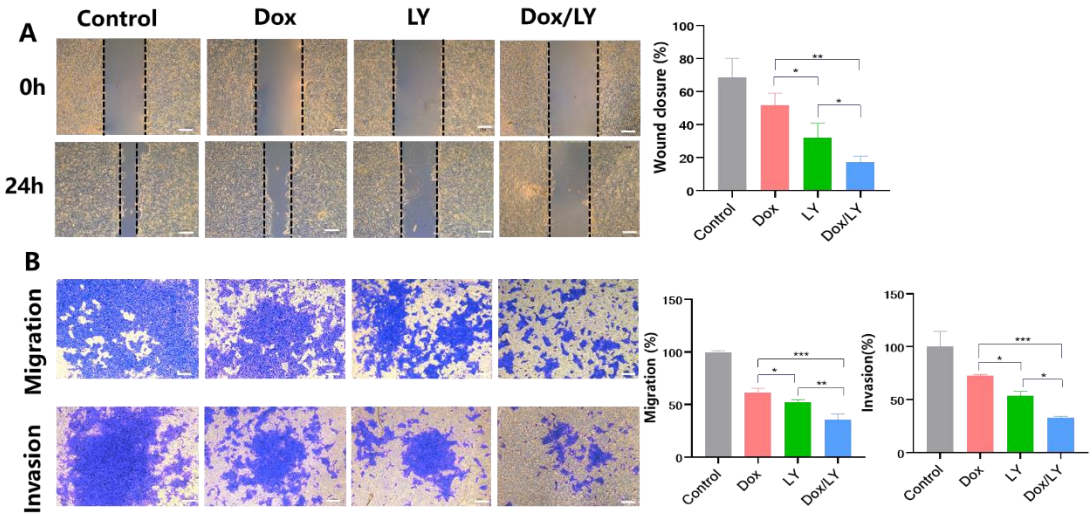

Fig.S8 *In vitro* anti-metastasis efficacy of free drugs after indicated treatments. (A) Representative images of wound healing and relative wound healing rate; (B) representative images of transwell, relative migration and invasion rate. (Scale bars: 200 μm; n = 3, **p* < 0.05, ***p* < 0.01, ****p* < 0.001)

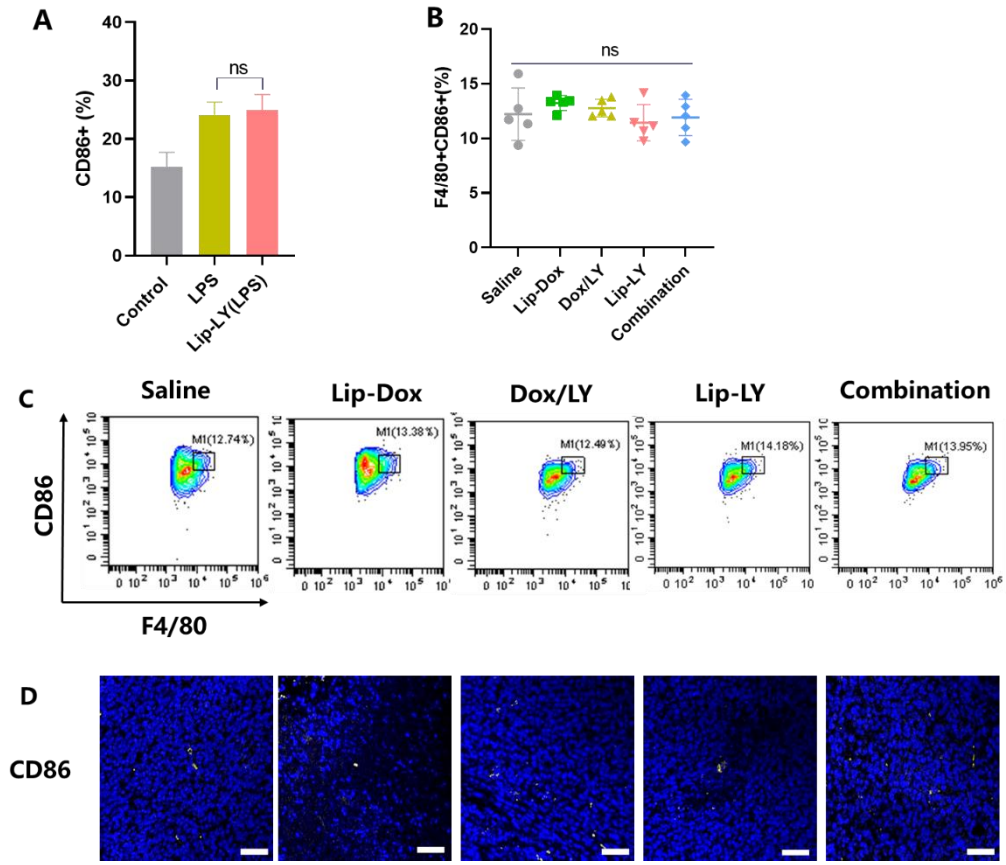

Fig. S9 The effect of combination treatment on M1 TAMs. (A) Flow cytometry analysis of CD86 in BMDM (n=3). (B) Flow cytometry analysis of M1 TAMs ($F4/80^{+}CD206^{+}$ cells) in 4T1 tumors after indicated treatments (n=5). (C) Representative flow cytometry profiles of M1 TAMs. (D) Immunofluorescence staining of M2 TAMs in 4T1 tumors after different treatments (Scale bar: 50 μm, ns: p >0.05).

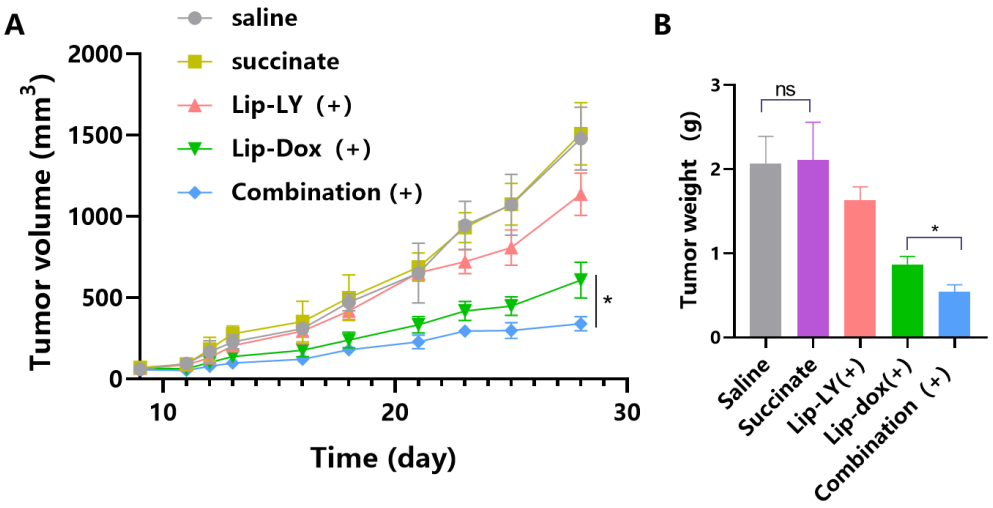

Fig. S10 Antitumor activity of combination treatment in 4T1 tumor-bearing BALB/c mice. (A) Tumor growth curve and (B) Tumor weight of 4T1 tumor-bearing BALB/c mice after indicated treatments (n=5, ns: $p > 0.05$, *$p < 0.05$, "+" means succinate stimulation).